Statistics and Dynamics of the Center-of-Mass Coordinate in a Quantum Liquid

Balázs Dóra,[1,*] Balázs Hetényi,[2] and Cătălin Paşcu Moca[2,3]
[1]Department of Theoretical Physics and MTA-BME Lendület Topology and Correlation Research Group, Budapest University of Technology and Economics, 1521 Budapest, Hungary
[2]Department of Theoretical Physics and BME-MTA Exotic Quantum Phases Research Group, Budapest University of Technology and Economics, 1521 Budapest, Hungary
[3]Department of Physics, University of Oradea, 410087 Oradea, Romania

(Received 29 April 2018; revised manuscript received 29 June 2018; published 2 August 2018)

Motivated by recent experiments in ultracold gases, we focus on the properties of the center-of-mass coordinate of an interacting one-dimensional Fermi gas, displaying several distinct phases. While the variance of the center of mass vanishes in insulating phases such as phase-separated and charge density wave phases, it remains finite in the metallic phase, which realizes a Luttinger liquid. By combining numerics with bosonization, we demonstrate that the autocorrelation function of the center-of-mass coordinate is universal throughout the metallic phase. It exhibits persistent oscillations, and its short time dynamics reveal important features of the quantum liquid, such as the Luttinger liquid parameter and the renormalized velocity. The full counting statistics of the center of mass follows a normal distribution already for small systems. Our results apply to nonintegrable systems as well and are within experimental reach for, e.g., carbon nanotubes and cold atomic gases.

DOI: 10.1103/PhysRevLett.121.056803

Introduction.—Strong correlations in combination with quantum mechanics in reduced dimensions have already provided a plethora of fascinating phenomena [1,2], including spin-charge separation, charge fractionalization, Wigner crystals, and non-Fermi liquid behavior. Many of these pop up in a variety of fermionic and bosonic systems, including condensed matter, cold atomic systems [3], quantum optics [4], and even in black holes [5]. Not only compelling, these systems promise to be relevant for possible application in topological quantum computation, spintronics, and quantum information theory.

In classical mechanics, the concept of the center-of-mass coordinate plays a prominent role. Because of Newton's third law, the action and reaction forces between the particles compensate each other, and the center of mass is influenced only by external forces. The very same program can also be carried out in quantum mechanics, and the center-of-mass coordinate gets separated from the relative ones [6]. However, this works only when the interaction depends on the relative position of the particles and not on their absolute position. In any realistic setting in condensed matter or cold atomic systems, an atomic or trapping potential is inevitably present, involving the absolute position of particles. Therefore, the center-of-mass contribution cannot be separated from the rest, and its properties are influenced by strong correlations. Understanding how this happens is the main goal of this work, and low-dimensional quantum systems featuring enhanced correlation effects represent an ideal playground for that.

The proper definition of the many-body position or center-of-mass coordinate has a long history [7,8], especially with periodic boundary conditions. With open boundary conditions (OBCs), however, one can legitimately define the position operator in the conventional way [9] as $\sum_i x_i$ by summing over the position operator of each particle. Moreover, experimental realizations often imply OBCs. In this context, a recent experiment on weakly interacting bosons in one dimension has already investigated the dynamics of the center of mass [10]. Our aim is to shed light on the complementary, strongly correlated side of the problem; thus, we focus on a strongly interacting one-dimensional quantum liquid in one dimension with OBC [11]. We find that the center-of-mass coordinate reveals universal behavior and its variance vanishes in insulating phases. In the Luttinger liquid (LL) phase, its variance gives a direct measure of the LL parameter. Its temporal dynamics follows a universal scaling function and reveals the other relevant parameter of the low-energy theory, the renormalized velocity. The full counting statistics of the center of mass obey a normal distribution already for small systems with 8–10 particles. The observation of all these features is within experimental reach.

Interacting fermions in 1D: Lattice and continuum.—We study one-dimensional spinless fermions in a tight-binding chain with nearest-neighbor interaction at half filling and OBC [12] using several numerical techniques. This problem is equivalent to the 1D Heisenberg XXZ chain after a Jordan-Wigner transformation [1,2]. The Hamiltonian is

$$H = \sum_{m=1}^{N-1} \left[\frac{J}{2} (c_{m+1}^{\dagger} c_m + c_m^{\dagger} c_{m+1}) + J_z n_{m+1} n_m \right], \quad (1)$$

 © 2018 American Physical Society

where c's are fermionic operators, $n_m = c_m^\dagger c_m$, J_z denotes the nearest-neighbor repulsion and N the number of lattice sites, and the model hosts $N/2$ fermions. This model realizes a Luttinger liquid for $|J_z| < J$, and the strength of the interaction is characterized by the dimensionless LL parameter [1] $K = \pi/2[\pi - \arccos(J_z/J)]$ and renormalized velocity $v = aJ\pi\sqrt{1-(J_z/J)^2}/2\arccos(J_z/J)$ with a the lattice constant. For $J_z > J$, the ground state becomes a charge density wave through a Kosterlitz-Thouless transition with broken Z_2 (corresponding to even and odd lattice sites) symmetry, while for $J_z < -J$, the ground state is phase separated through a first-order phase transition; i.e., all $N/2$ fermions are "bound" together. This model is solved using exact diagonalization (ED) with a Lanczos algorithm up to $N = 26$ and by the density matrix renormalization group (DMRG) up to $N = 80$.

The low-energy effective field theory of Eq. (1) in the LL phase is obtained using Abelian bosonization [1–3], capturing interaction effects nonperturbatively. Using this procedure, the LL phase of this model with OBCs is mapped onto [11,13]

$$H = \sum_{q>0} \omega(q) b_q^\dagger b_q, \tag{2}$$

where b_q accounts for the density fluctuations [1] of the fermions in Eq. (1) and the long wavelength part of the local charge density is $\rho(x) = \partial_x \Theta(x)/\pi$ with

$$\Theta(x) = i\sum_{q>0} \sqrt{\frac{\pi K}{qL}} \sin(qx)[b_q - b_q^\dagger] \tag{3}$$

for the OBC, K the LL parameter, and $\omega(q) = vq$ with v the Fermi velocity in the interacting systems and $q = l\pi/L$ with $l = 1, 2, 3, \ldots$, and L is the system size.

Center of mass.—We define the dimensionless center-of-mass operator for Eq. (1) as [14]

$$\hat{x} = \frac{1}{N}\sum_{m=1}^{N}\left(m - \sum_{m'=1}^{N}\frac{m'}{N}\right) n_m, \tag{4}$$

where, for simplicity, we have subtracted the equilibrium position of the center-of-mass coordinate such that $\langle \hat{x} \rangle = 0$, irrespective of how the lattice sites are numbered. For identical particles (which we consider here), it is independent from their mass. This operator is also the normalized polarization operator [15]. Using bosonization, the very same quantity reads as

$$\hat{x} = \int_0^L \frac{dx}{\pi L} x \partial_x \Theta(x), \tag{5}$$

and we have neglected fast oscillating terms in the integrand [1–3] from short wavelength density fluctuations, which are expected to average out after the integral.

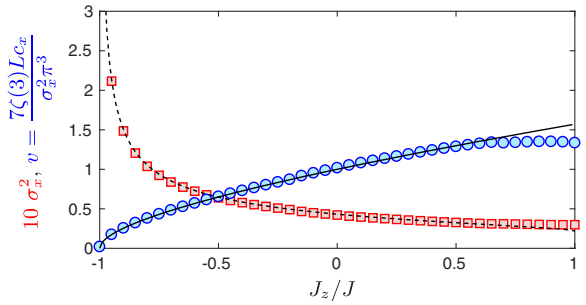

FIG. 1. The variance (red squares) of the center of mass and the LL velocity (blue circles) in Ja units from the center-of-mass autocorrelator are plotted from DMRG with $N = 80$. The analytical results from Eqs. (6) and (8) using the Bethe ansatz results for K and v without any fitting parameter are shown by black lines.

While the expectation value of the center-of-mass operator is zero, its standard deviation σ_x reads as

$$\sigma_x^2 = \langle \hat{x}^2 \rangle = \int_0^L dx \int_0^L dy \frac{xy\langle \partial_x\Theta(x)\partial_y\Theta(y)\rangle}{\pi^2 L^2}$$
$$= \sum_{q>0} \frac{Kq}{\pi L}\left[\int_0^L dx \cos(qx)\frac{x}{L}\right]^2 = \frac{7\zeta(3)}{2\pi^4}K, \tag{6}$$

where $\zeta(z)$ is the Riemann zeta function [16] and $\zeta(3) \approx 1.202$. The σ_x is universal in the sense that it depends only on the LL parameter K but is independent of the high-energy degrees of freedom: Very different microscopic Hamiltonians with the same LL parameter possess identical σ_x. Since K decreases with increasing J_z, this implies that, counterintuitively, the variance gets suppressed when moving from the attractive to the repulsive side. The numerical results from DMRG agree very nicely with Eq. (6), as seen in Fig. 1. The variance diverges as $\sigma_x^2 \sim \sqrt{J/(J+J_z)}$ at the first-order critical point. Slight deviations are visible close to $J_z \sim J$, arising from the terms in the Hamiltonian, driving the Kosterlitz-Thouless transition, which are missing from Eq. (2). Nevertheless, the variance seems to remain finite at this critical point.

The above calculation can be extended to the gapped charge density wave phase, when the effective field theory of Eq. (1) is the sine-Gordon model [1,2]. In this case, a Mott gap Δ opens up in the spectrum. Within the realm of the semiclassical limit of this model, following Refs. [17,18], the variance of the center of mass is calculated with K replaced by $\omega(q)/\sqrt{\omega^2(q)+\Delta^2}$ in Eq. (6) under the sum. This gives $\sigma_x^2 \sim v/L\Delta$ and vanishes in the thermodynamic limit, which is also corroborated by ED. For finite systems, the variance vanishes when the system size L is much longer than the correlation length v/Δ. Alternatively, the variance is negligible when the level spacing v/L is much smaller than the actual gap [19].

In the phase-separated regime, bosonization is not applicable, but the variance of the center of mass can be

calculated. Since all $N/2$ particles are bound together by the strong attractive interaction in the lattice of N sites, the ground state is, in principle, highly degenerate. As a result, $\sigma_x \sim N/2$, which agrees with ED results on clean systems. However, any disorder or imperfection in the lattice, which is inevitably present in any real system, breaks this degeneracy and produces a unique ground state. Therein, the $N/2$ particles occupy neighboring lattice sites, their position is well defined, and the variance is zero, as we also find from ED in the presence of weak impurities or disorder.

Dynamics of the center of mass.—To gain further insight into the behavior of the center-of-mass operator, we evaluate its autocorrelation function as $\chi_x(t) = \langle \hat{x}(t)\hat{x}(0)\rangle$. Using $b_q(t) = b_q \exp(-i\omega(q)t)$ in Eq. (3), we obtain

$$\chi_x(t) = \frac{2K}{\pi^4}\sum_{l=1}^{\infty}\frac{1-(-1)^l}{l^3}\exp(-ivt\pi l/L) = \frac{2K}{\pi^4}\sum_{b=\pm} b\,\mathrm{Li}_3(b\,\exp(-ivt\pi/L)), \tag{7}$$

with $\mathrm{Li}_s(z)$ the polylogarithm function, and $\chi_x(0) = \sigma_x^2$. Although Eq. (7) looks complicated at first, it is rather well approximated by $\chi_x(t) \approx \sigma_x^2 \exp(-ivt\pi/L)$. Similarly to the variance of the center of mass, $\chi_x(t)$ is also independent of any cutoff and depends only on the universal combination vt/L. Its initial temporal slope is

$$c_x = i\partial_t\chi_x(t\to 0) = \langle[\hat{x}, H]\hat{x}\rangle = \frac{1}{2\pi L}vK, \tag{8}$$

which depends only on the LL parameter K and the renormalized velocity of the interacting theory. Therefore, by measuring the variance of the center of mass and its initial dynamics, one can easily extract the two and only two essential ingredients of the LL theory, the velocity from $v = 7\zeta(3)Lc_x/\sigma_x^2\pi^3$ and the LL parameter from σ_x, as shown in Fig. 1. In addition, Eq. (7) predicts a universal data collapse of the center-of-mass oscillation; namely, upon rescaling its magnitude by $1/K$ and its temporal evolution by v/L, all curves should fall on top of each other, irrespective of the strength or even the sign of the interaction, as shown in Fig. 2. The time dependence spans several N/J periods (with $N = 26$), and the agreement between numerics and Eq. (7) remains excellent, even though K and v decrease or increase by more than a factor of 2 from $J_z/J = -0.6$ to 0.6, respectively.

The center-of-mass autocorrelator is found to be universal at all timescales. This is somewhat surprising, since the LL theory is designed to capture the low-energy physics, and thus it is expected to be universal in the long time limit. For $\chi_x(t)$, on the other hand, already the short time dynamics turns out to be universal. The lattice model in Eq. (1) is integrable [1,2]; therefore, one may wonder whether these persistent oscillations arise due to the large

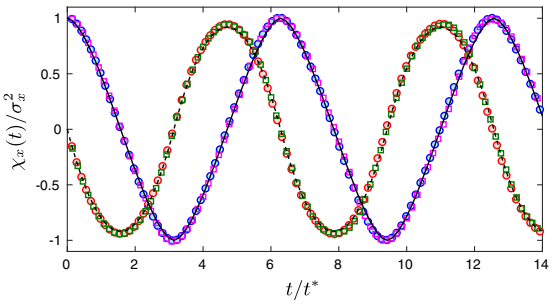

FIG. 2. Demonstration of the data collapse for LL with strong attraction and repulsion. The real (black solid curve) and imaginary (black dash-dotted curve) parts of the center-of-mass autocorrelator are plotted from Eq. (7) with $t^* = L/v\pi$, together with the numerical data from ED for $N = 26$ and $J_z/J = 0.6$ (circle) and -0.6 (square), normalized to the corresponding variance. The only fit parameter for ED is the horizontal timescale, satisfying $t^* \sim L/v\pi$.

number of constants of motion. Integrability is destroyed by adding a second nearest-neighbor density-density (i.e., $J_z'\sum_m n_{m+2}n_m$) interaction [20], which we have also studied numerically for several J_z and J_z', yielding identical results to the integrable case: The persistent oscillations from Eq. (7) remain intact also for nonintegrable LLs.

Persistent oscillation shows up in the Calogero-Sutherland model [21] as well, sensitive to the trapping frequency. This is argued to be a specific feature following from the integrability of the model and its long-range interaction. The persistent oscillation in Eq. (7) is analogous to this and scales with the "trapping frequency" $v\pi/L$ from the OBC. The OBC can also arise from a sharp box trapping potential [22,23]. However, the LL description applies to a large variety of systems, including fermions, bosons, spins [3], etc. Therefore, the persistent oscillation is expected to be a generic feature in these models, irrespective of the microscopic details.

Full counting statistics.—Already, simple expectation values of physical quantities often display rather complex behavior. Higher moments of the observables contain, however, infinitely more information and encode unique information about, e.g., nonlocal, multipoint correlators and entanglement, though they are typically difficult to access. Their information content is equivalent to determining the full distribution function of the quantity of interest.

Having studied simple correlation functions of the center-of-mass coordinate, we now address its full counting statistics [24–27]. Its probability distribution function is

$$P(X) = \langle\delta(X - \hat{x})\rangle, \tag{9}$$

whose characteristic function can easily be evaluated to yield $G(p) = \langle\exp(i\hat{x}p)\rangle$. Note that $G(p)$ is reminiscent of how the polarization operator is defined [7,8,28] for a periodic boundary condition, using only integer multiples of 2π for p. Here, on the contrary, p takes any real values in the characteristic function, and the normalized position and

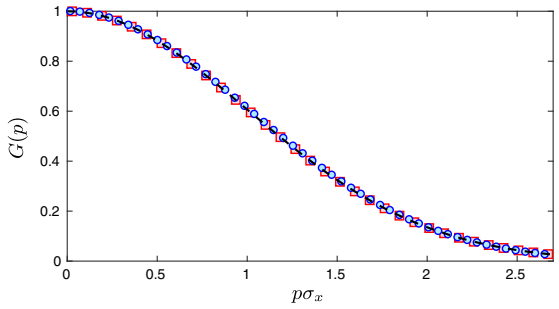

FIG. 3. Characteristic function of the center-of-mass coordinate from bosonization (dashed line) together with the numerical data from ED after finite size scaling to $N \to \infty$ using $N = 14$, 18, 22, and 26 and $J_z/J = 0.6$ (circle) and -0.6 (square).

polarization operator $\hat{x}$ is defined by Eq. (4) without any ambiguity [9].

Since $\hat{x}$ in the exponent is a linear function of bosonic operators and the low-energy Hamiltonian is quadratic in Eq. (2), the expectation value is evaluated as [29]

$$G(p) = \exp(-p^2\langle\hat{x}^2\rangle/2) = \exp(-p^2\sigma_x^2/2). \quad (10)$$

This is calculated also for Eq. (1) numerically using ED after finite size scaling and plotted in Fig. 3, revealing excellent agreement between Eq. (10) and the numerical data. For smaller systems and especially for repulsive $J_z \sim J$, slight deviations show up from the Gaussian behavior for large p, which stem from the fact that $\|\hat{x}\| < N/2$ is bounded for finite systems; therefore, deviations appear in the tail, which diminish upon increasing the system size. Its Fourier transform gives the probability distribution function as a normal distribution with variance σ_x^2 as $P(X) = (1/\sqrt{2\pi}\sigma_x)\exp[-(X^2/2\sigma_x^2)]$. The normal distribution itself is expected from the central limit theorem in the thermodynamic limit. However, on the one hand, it is surprising that already for small system sizes, where higher moments could, in principle, deviate from Gaussianity, the numerical data approach it very fast for systems with 8–10 particles, especially for attractive interactions. The same distribution applies for attractive Bose-Einstein condensates in a harmonic trap [30]. On the other hand, in contrast to the smooth, almost N-independent behavior of $G(p)$ for the OBC and its nice agreement with bosonization in Fig. 3, the very same quantity exhibits power law size dependence for a *periodic* boundary condition as $G(p) \sim N^{-\alpha(p)}$ and the exponent $\alpha(p)$ does not follow the field theory prediction [28].

Experimental ramifications.—There exists well-developed experimental technology to observe these effects. LLs are routinely realized in both cold atomic settings, using spins, bosons, or fermions, and condensed matter systems [3], including, e.g., carbon nanotubes, described identically by Eq. (2). The center-of-mass coordinate can be monitored using time of flight imaging [31], *in situ* absorption imaging [10], or scanning tunneling microscopy [32], allowing for the observation of its variance as well as its full distribution function or at least some of its lower moments. These are all universal quantities, depending on the interaction only through the LL parameter K. This is tunable by changing the lattice parameters or tuning the Feshbach resonance for cold atoms in a wide range, while the interaction in condensed matter is controllable by tuning the relative permittivity of the surrounding material.

The dynamics of the center-of-mass coordinate is measurable by, e.g., tilting the lattice or applying a weak electric field at time $t = 0$, represented by the scalar potential of the force F, which creates a perturbation $H' = L\hat{x}F(t)$ as in Refs. [33,34]. Then, within the linear response theory, the motion of the center of mass follows as

$$\langle\hat{x}(t)\rangle = -2L\int_0^t dt' \mathrm{Im}\chi_x(t-t')F(t'). \quad (11)$$

For short times, $\mathrm{Im}\chi_x(t) = -vKt/2\pi L$, revealing the two LL characteristics in a universal manner. Therefore, initially $\langle\hat{x}(t)\rangle = vKt^2F/2\pi$ after switching on a constant force F, corresponding to the classical motion of a particle in an external force F with "mass" $\sim\pi/vK$. Based on Eq. (7) and Fig. 2, the $\langle\hat{x}(t)\rangle$ will exhibit persistent oscillations for longer times with frequency $v\pi/L$. At the same time, the variance of the oscillating center of mass remains unchanged, and it does not spread during the oscillations, in spite of being built up from many distinct dispersive modes. Note that Eq. (11) is *exact* within the realm of bosonization; there are no higher-order corrections in F. This follows from the linear dispersion in $\omega(q) \sim q$, extending up to infinitely large energies, without any band bending. This is completely analogous to how the Born scattering limit of the Dirac-delta potential is exact for the same linear dispersion [2].

The experimental setup in Ref. [10] can be readily used to investigate these predictions. Therein, a weakly interacting Bose gas of ^{7}Li was monitored, and the dynamics of its center of mass was measured in the presence of a strong driving force, while our results apply in the opposite case of a strong interaction and weak driving field, which is realizable experimentally. In a related experiment [35], the center of mass of noninteracting ^{7}Li particles was measured in an excited band, but interactions can be induced by making use of its Feshbach resonances [36]. Our fermionic model in Eq. (1) can equally be realized in terms of hard core bosons [1], which corresponds to the Tonks-Girardeau limit of a 1D Bose gas [37], created from ^{87}Rb. The dynamics of the center of mass is accessible following Refs. [10,35].

The dynamics of the center of mass is reminiscent of Bloch oscillations [33,38], which also arise in the presence of an external force, albeit the persistent oscillations in Eqs. (7) and (11) arise in a strongly correlated quantum liquid as opposed to the standard single-particle picture behind Bloch oscillations [38]. The analogy with Bloch oscillations is extended by noting that the reflection on the

boundary of the lattice in our study plays the role of a Bragg reflection at the boundary of the Brillouin zone in the case of Bloch oscillations. The typical timescale of Bloch oscillations, $t_B = 1/aF$ with a the lattice constant, represents the time during which the full Brillouin zone is swept through by the force, while the timescale for the center-of-mass oscillation due to finite size effects from Eq. (7) is L/v, i.e., the timescale for sweeping through the real space lattice. Our results are observable on the timescale of $t \sim L/v \ll t_B$ before Bloch oscillations set in, requiring weak forces in Eq. (11) and, more importantly, small systems, which suits ideally the experimental conditions.

Conclusions.—We have demonstrated that the center-of-mass coordinate exhibits universal behavior in a Luttinger liquid and bosonization gives essentially exact results for *all* of its properties. Most importantly, the LL parameter can be directly measured using the variance of the center-of-mass coordinate. In combination with its short time dynamics, the other basic characteristic of the underlying quantum liquid, namely, the renormalized velocity, is revealed. The correlation function as well as the full counting statistics of the center-of-mass coordinate follow a universal function, which are corroborated by analytical and numerical methods. These are within experimental reach in both condensed matter and cold atomic realizations, using setups similar to Bloch oscillations.

We are grateful for useful discussions with I. Lovas. This research is supported by the National Research, Development and Innovation Office NKFIH within the Quantum Technology National Excellence Program (Project No. 2017-1.2.1-NKP-2017-00001) and Grant No. K119442, and by the Romanian National Authority for Scientific Research and Innovation, UEFISCDI, Project No. PN-III-P4-ID-PCE-2016-0032.

*dora@eik.bme.hu

[1] T. Giamarchi, *Quantum Physics in One Dimension* (Oxford University, New York, 2004).
[2] A. O. Gogolin, A. A. Nersesyan, and A. M. Tsvelik, *Bosonization and Strongly Correlated Systems* (Cambridge University Press, Cambridge, England, 1998).
[3] M. A. Cazalilla, R. Citro, T. Giamarchi, E. Orignac, and M. Rigol, One dimensional bosons: From condensed matter systems to ultracold gases, Rev. Mod. Phys. **83**, 1405 (2011).
[4] D. E. Chang, V. Gritsev, G. Morigi, V. Vuletic, M. D. Lukin, and E. A. Demler, Crystallization of strongly interacting photons in a nonlinear optical fibre, Nat. Phys. **4**, 884 (2008).
[5] V. Balasubramanian, I. García-Etxebarria, F. Larsen, and J. Simón, Helical Luttinger liquids and three-dimensional black holes, Phys. Rev. D **84**, 126012 (2011).
[6] A. Messiah, *Quantum Mechanics*, Dover books on physics (Dover, New York, 1961).
[7] R. Resta, Quantum-Mechanical Position Operator in Extended Systems, Phys. Rev. Lett. **80**, 1800 (1998).
[8] R. Resta and S. Sorella, Electron Localization in the Insulating State, Phys. Rev. Lett. **82**, 370 (1999).
[9] M. Rigol and B. S. Shastry, Drude weight in systems with open boundary conditions, Phys. Rev. B **77**, 161101 (2008).
[10] Z. A. Geiger, K. M. Fujiwara, K. Singh, R. Senaratne, S. V. Rajagopal, M. Lipatov, T. Shimasaki, R. Driben, V. V. Konotop, T. Meier, and D. M. Weld, Observation and Uses of Position-Space Bloch Oscillations in an Ultracold Gas, Phys. Rev. Lett. **120**, 213201 (2018).
[11] M. A. Cazalilla, Bosonizing one-dimensional cold atomic gases, J. Phys. B **37**, S1 (2004).
[12] The OBC arises from a box trapping potential by using holographic masks [22] or by confining cold atoms in a ring lattice and cutting it open or by using gates to confine electrons in carbon nanotubes.
[13] M. Fabrizio and A. O. Gogolin, Interacting one-dimensional electron gas with open boundaries, Phys. Rev. B **51**, 17827 (1995).
[14] T. Vaughan, P. Drummond, and G. Leuchs, Quantum limits to center-of-mass measurements, Phys. Rev. A **75**, 033617 (2007).
[15] G. D. Mahan, *Many Particle Physics* (Plenum, New York, 1990).
[16] I. S. Gradshteyn and I. M. Ryzhik, *Table of Integrals, Series, and Products* (Academic, New York, 2007).
[17] K. Maki and H. Takayama, Quantum-statistical mechanics of extended objects. I. Kinks in the one-dimensional sine-Gordon system, Phys. Rev. B **20**, 3223 (1979).
[18] A. Iucci and M. A. Cazalilla, Quantum quench dynamics of the sine-Gordon model in some solvable limits, New J. Phys. **12**, 055019 (2010).
[19] This would allow for estimating the gap size from measuring the variance of the center of mass in finite size systems.
[20] K. Hallberg, E. Gagliano, and C. Balseiro, Finite-size study of a spin-1/2 Heisenberg chain with competing interactions: Phase diagram and critical behavior, Phys. Rev. B **41**, 9474 (1990).
[21] B. Sutherland, Exact Coherent States of a One-Dimensional Quantum Fluid in a Time-Dependent Trapping Potential, Phys. Rev. Lett. **80**, 3678 (1998).
[22] W. S. Bakr, J. I. Gillen, A. Peng, S. Fölling, and M. Greiner, A quantum gas microscope for detecting single atoms in a Hubbard-regime optical lattice, Nature (London) **462**, 74 (2009).
[23] A. L. Gaunt, T. F. Schmidutz, I. Gotlibovych, R. P. Smith, and Z. Hadzibabic, Bose-Einstein Condensation of Atoms in a Uniform Potential, Phys. Rev. Lett. **110**, 200406 (2013).
[24] L. S. Levitov, H. Lee, and G. B. Lesovik, Electron counting statistics and coherent states of electric current, J. Math. Phys. (N.Y.) **37**, 4845 (1996).
[25] V. Gritsev, E. Altman, E. Demler, and A. Polkovnikov, Full quantum distribution of contrast in interference experiments between interacting one-dimensional Bose liquids, Nat. Phys. **2**, 705 (2006).
[26] A. Silva, Statistics of the Work Done on a Quantum Critical System by Quenching a Control Parameter, Phys. Rev. Lett. **101**, 120603 (2008).
[27] M. Gring, M. Kuhnert, T. Langen, T. Kitagawa, B. Rauer, M. Schreitl, I. Mazets, D. A. Smith, E. Demler, and J. Schmiedmayer, Relaxation and prethermalization in an isolated quantum system, Science **337**, 1318 (2012).

[28] R. Kobayashi, Y. O. Nakagawa, Y. Fukusumi, and M. Oshikawa, Scaling of the polarization amplitude in quantum many-body systems in one dimension, Phys. Rev. B **97**, 165133 (2018).

[29] J. von Delft and H. Schoeller, Bosonization for beginners refermionization for experts, Ann. Phys. (Berlin) **7**, 225 (1998).

[30] K. Sakmann and M. Kasevich, Single-shot simulations of dynamic quantum many-body systems, Nat. Phys. **12**, 451 (2016).

[31] I. Bloch, J. Dalibard, and W. Zwerger, Many-body physics with ultracold gases, Rev. Mod. Phys. **80**, 885 (2008).

[32] A. Hamo, A. Benyamini, I. Shapir, I. Khivrich, J. Waissman, K. Kaasbjerg, Y. Oreg, F. von Oppen, and S. Ilani, Electron attraction mediated by Coulomb repulsion, Nature (London) **535**, 395 (2016).

[33] M. B. Dahan, E. Peik, J. Reichel, Y. Castin, and C. Salomon, Bloch Oscillations of Atoms in an Optical Potential, Phys. Rev. Lett. **76**, 4508 (1996).

[34] M. Gustavsson, E. Haller, M. J. Mark, J. G. Danzl, G. Rojas-Kopeinig, and H.-C. Nägerl, Control of Interaction-Induced Dephasing of Bloch Oscillations, Phys. Rev. Lett. **100**, 080404 (2008).

[35] K. M. Fujiwara, Z. A. Geiger, K. Singh, R. Senaratne, S. V. Rajagopal, M. Lipatov, T. Shimasaki, and D. M. Weld, Experimental realization of a relativistic harmonic oscillator, New J. Phys. **20**, 063027 (2018).

[36] C. Chin, R. Grimm, P. Julienne, and E. Tiesinga, Feshbach resonances in ultracold gases, Rev. Mod. Phys. **82**, 1225 (2010).

[37] B. Paredes, A. Widera, V. Murg, O. Mandel, S. F. I. Cirac, G. V. Shlyapnikov, T. W. Hänsch, and I. Bloch, Tonks-Girardeau gas of ultracold atoms in an optical lattice, Nature (London) **429**, 277 (2004).

[38] J. H. Davies, *The Physics of Low-Dimensional Semiconductors: An Introduction* (Cambridge University, Cambridge, England, 1997).